Superalloys 2004
Edited by K.A. Green, T.M. Pollock, H. Harada,
T.E. Howson, R.C. Reed, J.J. Schirra, and S. Walston
TMS (The Minerals, Metals & Materials Society), 2004

EFFECT OF MICROSTRUCTURE (AND HEAT TREATMENT) ON THE 649°C PROPERTIES OF ADVANCED P/M SUPERALLOY DISK MATERIALS

John J. Schirra and Paul L. Reynolds – Pratt & Whitney, East Hartford, CT
Eric S. Huron*, Kenneth R. Bain*, David P. Mourer** – General Electric Aircraft Engines *Cincinnati, OH; **Lynn, MA

Keywords: Microstructure, Properties, PM,Superalloy,Disk

Abstract

A statistically based approach was completed to assess the effect of microstructural (and associated heat treatment processing parameters) on the 649°C capability of two advanced powder metallurgy (P/M) superalloys. The results showed that microstructure and processing play a key role in achieving a balance of mechanical properties. For a desired combination of good high temperature capability the results indicate that a supersolvus heat treatment followed by a fast cooling rate is desired. In addition, selection of a stabilization heat treat cycle would depend upon the balance of creep and crack growth capability desired. The process described above would nominally produce an ASTM 6 grain size with reasonably fine cooling γ' and aging γ' as defined by the stabilization cycle.

Introduction

Development of advanced P/M superalloy disk materials has resulted in an overall maturity of the technology such that continued improvements will most likely result from systematic experimentation aimed at understanding the specific contributions from the various metallurgical effects including composition as well as processing and microstructure. In addition, insight provided by the development of physically based models (ref. 1) will help enable practitioners to optimize materials for specific applications. Previous work has indicated that the elevated temperature properties of superalloy disk materials are strongly influenced by grain size (ref. 2) and γ' distribution (ref. 3). Based in part on this a research program was undertaken as part of the NASA sponsored Enabling Propulsion Materials (EPM) program to study the effect of heat treat parameters and associated microstructure on the elevated temperature properties of two advanced P/M superalloy materials (ref 4) (KM4 and SR3). This was one of several tasks aimed at developing a detailed understanding of the effect of factors such as minor element (grain boundary) composition (ref. 5) on the balance of properties required for a long-time, high-temperature disk application as part of the NASA supported and industrially led (GEAE/P&W) EPM initiative. Activities reported in this paper were conducted to establish the effect of microstructural variations on the elevated temperature balance of properties. Microstructural features selected for evaluation included grain size, γ' size (cooling and aging) and cooling γ' fraction. Statistically designed test matrices were utilized to optimize the information gained. The approach selected was a Taguchi idle column L8 design that permits the evaluation of four variables, two variables at two experimental levels and two variables at three levels, without interactions between the main effects. The basic experimental matrix is presented in Table I. The research activity focused on two objectives; the first was to define the response of the advanced P/M superalloy materials to various thermal exposures to establish the required heat treatments necessary to achieve the targeted microstructures established for the experimental matrices and the second was to process and evaluate the material per the experimental matrix design and analyze the results.

Details

The alloys selected for the test program were state of the art P/M alloys matured as part of a Navy funded development program (ref. 6). The alloys resulted from research aimed at producing alloy compositions optimized for higher temperature applications and are designated KM4 and SR3. Material was produced at Homogeneous Metals, Inc. pilot plant facility in Clayville, New York using conventional P/M processing

Table I. Experimental Matrix Based on Taguchi L8 Idle Column Design

	Variable and Experimental Setting			
Run #	Variable 1	Variable 2	Variable 3	Variable 4
1	-	-	-	-
2	-	+	+	+
3	0	+	-	+
4	0	-	+	-
5	0	-	+	+
6	0	+	0	-
7	+	+	+	-
8	+	-	0	+

Approximately 45 kilograms of powder was placed into steel containers for subsequent hot compaction and extrusion at Wyman Gordon's facilities in Houston, Texas. Extrusion conversion resulted in a > 95% recrystallized fine grain size (ASTM 14). Compositions for the extruded material are presented in Table II. Forging mults (Figure 1) were machined from the

Table II. Aim and Actual Compositions for SR3 and KM4 Alloys Evaluated in the Microstructural Program

	SR3 (Weight %)		KM4 (Weight %)	
Element	Aim	Actual	Aim	Actual
Al	2.6	2.4	4	3.8
Ti	4.9	4.9	4	3.9
Nb	1.6	1.6	2	1.9
Co	11.9	11.8	18	18.3
Cr	12.8	13.2	12	12
Mo	5.1	5.1	4	4
B	.015	.016	.03	.03
Hf	.2	.23	-	-
C	.03	.03	.03	.03
Zr	.03	.04	.03	.04
Ni	Balance	Balance	Balance	Balance

extrusions and Gatorized™ at a temperature of 1065°C and strain rate of 0.0017 sec^{-1} at P&W's isothermal forging facilities in West Palm Beach, Florida to yield forgings approximately 19 cm in diameter by 2.5 cm thick (Figure 1). The pancake forgings were machined into small test cubes (~1 cubic centimeter) for heat treat development and into specimen blanks (~2.5 cm square x 13 cm long) for better uniformity of heat treat processing.

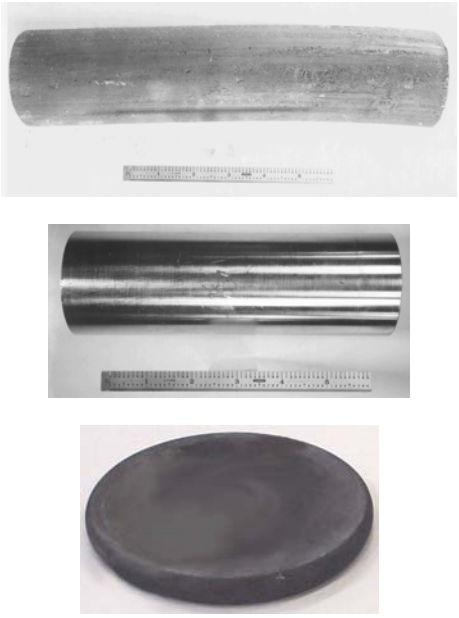

Figure 1
Typical Subscale Extrusion (top) and Forging Mult (middle) Used to Produce Experimental Forgings (bottom) for Microstructural Test Program

Levels selected for the experimental variables and assignment to the test matrices is presented in Table III. To define the heat treat parameters required to achieve the target microstructures it was necessary to establish the γ' solutioning and grain coarsening behavior as a function of temperature as well as the effect of cooling rate from solution heat treat on γ' size.

Table III. Target Microstructures for the Experimental Matrices.

Run #	Grain Size	Cooling γ' Size	Volume Fraction γ'	Stabilization Cycle
1	ASTM 4	.1 μm	50 %	None[1]
2	ASTM 4	.3 μm	100 %	843°C/4 hrs
3	ASTM 6	.3 μm	50 %	843°C/4 hrs
4	ASTM 6	.1 μm	100 %	None[1]
5	ASTM 6	.1 μm	100 %	843°C/4 hrs
6	ASTM 6	.3 μm	70 %	None[1]
7	ASTM 8	.3 μm	100 %	None[1]
8	ASTM 8	.1 μm	70 %	843°C/4 hrs

1) For the KM4 matrix, these runs were processed through a 1088°C/2 hours solution cycle.

To establish SR3 and KM4 γ' solutioning behavior test cubes were placed into an air furnace and heat treated at 1177°C for 24 hours. The material was then slow cooled to various temperatures (Table IV), removed from the furnace and rapid cooled to room temperature. The objective was to precipitate the γ' stable as very coarse precipitates during the slow cool with the γ' in solution precipitated as fine particles during the rapid cool. Samples were prepared with standard metallographic techniques and γ' etched for subsequent image analysis. At temperatures of 1093°C and above sufficient contrast was present to permit automatic measurement of area % γ' while below 1093°C a 144 point grid overlay / point count technique was used. Typical microstructures observed are presented in Figure 2. Up to

Table IV. Area Fraction γ' for KM4 (top) and SR3 (bottom).

End Temp[1]	Area % γ'	Measurements
1163°C	3.8 +/- .9	2.38, 2.79, 2.83, 3.33, 3.89, 4.22, 4.52, 4.53, 4.64, 4.71
1149°C	9.6 +/- 1.5	7.23, 8.35, 8.48, 9.37, 9.52 9.74, 9.93, 10.28, 11.02, 12.52
1135°C	13 +/- 1.1	10.54, 12.08, 12.27, 12.95, 13.21, 13.24, 13.65, 13.69, 13.79, 14.37
1121°C	16.6 +/- 1	14.5, 15.87, 16.17, 16.18, 16.43, 16.56, 17.12, 17.4, 17.6, 18.1
1107°C	21.8 +/- 3	14.06, 20.43, 21.49, 21.69, 21.82, 22.33, 22.54, 24.14, 24.35, 24.65
1093°C	25.2 +/- 1.4	23.11, 23.18, 24.09, 24.87, 25.39, 25.44, 25.75, 26.13, 26.62, 27.34
1037°C[2]	37.7+/-2.4	35.07, 36.81, 37.16, 37.85, 41.67,
871°C[2]	54.2+/-2.4	50.69, 53.13, 54.86, 55.56, 56.94

(KM4)

End Temp[1]	Area % γ'	Measurements
1163°C	NM	None observable
1149°C	7.9 +/- 1.1	6.34, 6.99, 7.03, 7.06, 7.54, 7.88, 8.21, 9.13, 9.48, 9.54
1135°C	9.9 +/- 1.6	7.98, 8.33, 8.45, 8.94, 9.2, 10.49, 10.61, 10.65, 12.26, 12.49
1121°C	14.4 +/- 1.7	11.46, 11.78, 13.61, 14.29, 14.58, 14.71, 15.47, 15.53, 15.88, 16.65
1107°C	17.9 +/- 1.6	15.16, 15.99, 17.24, 17.65, 17.77, 17.97, 18.59, 19.45, 19.72, 19.88
1093°C	21.2 +/- 2.4	17.87, 19.65, 19.73, 20.28, 20.5, 20.57, 20.58, 22.64, 23.63, 26.3
1037°C[2]	29.7 +/- 1.6	27.43, 28.82, 29.86, 30.9, 31.25
871°C[2]	49.2 +/- 2.8	46.53, 46.88, 48.61, 50.69, 53.13

(SR3)

1) Temperature when removed from furnace.
2) Measured using a grid overlay/point count technique.

10 fields of view were measured. Results (area %) are presented in Table IV and Figure 3. Total volume fraction contents were consistent with previous estimates for the alloys.

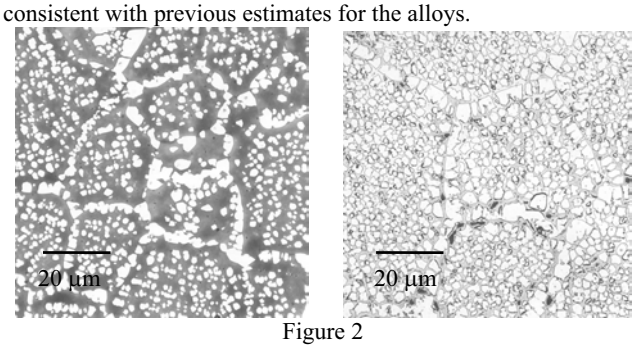

Figure 2
Typical Microstructures Slow Cooled to 1093 (left) and 871°C (right).

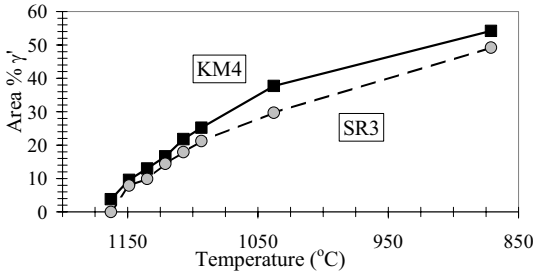

Figure 3
Measured Area % γ' as a Function of Temperature for KM4 & SR3

To establish the grain coarsening behavior, cubes were processed with and without a pre-heat treat anneal prior to the grain coarsening exposure. SR3 was heat treated at 1149°C for 1 hour followed by a furnace ramp to temperatures over the range 1171 to 1191°C for SR3. Material was also processed through 2 hour exposures over the temperature range 1149 to 1166°C followed by an air cool without the use of a preheat cycle. KM4 was heat treated with an 1135°C/2 hour cycle followed by a furnace ramp to temperatures over the range 1160 to 1185°C holding for 2 hours followed by an air cool. Additional material was also processed without the preheat cycle at temperatures over the range 1143 to 1199°C in 5.6°C increments for 2 hours followed by an air cool. Specimens were prepared using standard metallographic techniques and grain size measured using the Heyn-Intercept technique with a minimum of 50 intercepts counted per specimen. Results are listed in Tables V (KM4) and VI (SR3) and

Table V. Grain Coarsening of KM4. Intercept Distance in Italics. (Table is continued in the next column)

Temp[1]	Average	ASTM GS *(Intercept Distance (μm))*
1143°C	11.6 +/- 0.1 *(5.77+/-0.28)*	11.72,11.56,11.72,11.56,11.38 *(5.51,5.82,5.51,5.82,6.18)*
1149 °C	11.3 +/- 0.2 *(6.55 +/- .35)*	11.01,11.3,11.21,11.43,11.16 *(7.03,6.37,6.57,6.08,6.68)*
1154 °C	10.7 +/- .2 *(7.93 +/- .68)*	11.01,10.8,10.4,10.69,10.47 *(7.04,7.56,8.69,7.85,8.5)*
1160 °C	9.9 +/- .2 *(9.94 +/- .67)*	9.86,9.79,10.08,10.28,9.79 *(10.47,10.74,9.72,9.07,9.72)*
1160 °C[2]	9.9 +/- 0.1 *(10.6 +/- 0.7)*	9.8, 9.89, 9.85, 10.15, 9.89 *(11.21, 10.64, 10.92, 9.43, 10.64)*
1166 °C[2]	8.8 +/- 0.2 *(15.3 +/- 1.1)*	8.54, 8.66, 8.87, 8.77, 9.07 *(16.59, 15.95, 14.81, 15.36, 13.83)*
1166 °C [2]	9.2 +/- .3 *(13.25 +/- 1.22)*	8.8,9.2,9.11,9.47,9.38 *(15.12,13.17,13.61,12,12.37)*
1168 °C [2]	7 +/- 0.3 *(26.7 +/- 3.4)*	6.67, 6.87, 7.49, 6.87, 6.87 *(31.33, 29.49, 23.87, 24.49, 24.49)*
1171 °C [2]	6.2 +/- 0.3 *(37.8 +/- 4.2)*	6.38, 6.38, 6.45, 6.15, 5.66 *(35.68, 35.68, 34.49, 38.33, 44.99)*
1171 °C	8.2 +/- .2 *(20.1 +/- 1.58)*	8.08,7.94,7.63,8.21,8.08 *(19.44,20.41,22.68,18.55,19.4)*
1174 °C [2]	6.5 +/- 0.4 *(34.1 +/- 4.4)*	6.36, 7.05, 6.67, 6.25, 6.13 *(35.81, 27.85, 31.33, 37.13, 38.56)*
1177 °C [2]	5.7 +/- 0.5 *(45.8 +/- 8.4)*	6.26, 6.15, 4.95, 5.53, 5.41 *(36.96,38.33,57.49,47, 49.28)*
1177 °C	7.4 +/- .3 *(25.05 +/- 2.12)*	7.11,7.29,7.29,7.29,7.79 *(27.21,25.51,25.51,25.5,21.48)*
1182 °C[2]	5.6 +/- 0.4 *(46.2 +/- 6.9)*	5.41, 5.41, 5.13, 6.02, 6.15 *(49.28, 49.28, 54.46, 39.8, 38.33)*
1182 °C	7.3 +/- 0.4 *(24.35 +/- 3.28)*	7.47,7.63,6.91,7.94,7.29 *(24.01,22.68,29.16,20.41,25.5)*
Temp[1]	Average	ASTM GS *(Intercept Distance (μm))*
1185 °C[3]	6 +/- 0.4 *(40.2 +/- 6.2)*	5.88, 6.13, 5.36, 6.45, 6.36 *(41.78, 38.56, 50.13, 34.57, 35.81)*
1188 °C	7.6 +/- 0.4 *(22.79 +/- 3.65)*	7.94,7.94,7.79,7.64,6.91 *(20.38,20.38,21.45,22.64,29.1)*
1193 °C	7.3 +/- 0.5 *(24.77 +/- 4.14)*	7.3,7.47,7.94,6.7,7.64 *(25.48,23.98,20.38,31.35,22.6)*
1199 °C	7.0 +/- 0.4 *(28.4 +/- 4.08)*	7.64,6.91,7.11,6.47,6.91 *(22.64,29.11,27.17,33.97,29.1)*

1) Grain coarsening heat treat temperature.
2) Processed with a subsolvus anneal prior to grain coarsening exposure.

Table VI. Grain Coarsening of SR3. Intercept Distance in Italics.

Temp[1]	Average	ASTM GS *(Intercept Distance (μm))*
1149 °C	12.2 +/- .2 *(4.69 +/- .3)*	11.96, 12.19, 12.19, 12.4 *(5.07, 4.68, 4.68, 4.34)*
1154 °C	12.2 +/- .3 *(4.72 +/- .5)*	11.96, 11.96, 12.19, 12.6 *(5.07, 5.07, 4.68, 4.05)*
1160 °C	11.8 +/- .3 (5.34 +/- .6)	11.43, 11.71, 11.96, 12.19 (6.08, 5.53, 5.07, 4.68)
1166 °C	11 +/- .4 *(7.08 +/- 1)*	10.4,10.8,10.9,11.1,11.4,11.4 *(8.69,7.60,7.29,6.76,6.08,6.1)*
1171 °C	8 +/- .8 *(20.94 +/- 5.57)*	6.8,7.4,7.4,7.9,7.9,8.8,8.8,8.8 *(30.83, 24.66, 24.66, 20.55, 20.55, 15.41, 15.41, 15.41)*
1177 °C [2]	6.4 +/- .6 *(37.25 +/- 12.5)*	5.31, 6.34, 6.61, 6.86, 6.86 *(59.21, 35.53, 32.3, 29.61, 29.61)*
1182 °C [2]	5.6 +/- .5 *(45.56 +/- 9.02)*	4.86, 4.86, 5.31, 5.69, 5.69, 6.03, 6.03, 6.34 *(59.21, 59.21, 50.75, 44.41, 44.41, 39.47, 39.47, 35.53)*
1191 °C [2]	5.4 +/- .8 *(50.91 +/- 13.31)*	4.34,4.86,4.86,5.31,5.69,6,6.6 *(71.05, 59.21, 59.21, 50.75, 44.41, 39.47, 32.3)*

1) Grain coarsening heat treat temperature.
2) Processed with a subsolvus anneal prior to grain coarsening exposure.

summarized in Figure 4. Review of the grain coarsening results suggests that use of the preheat cycle results in the development

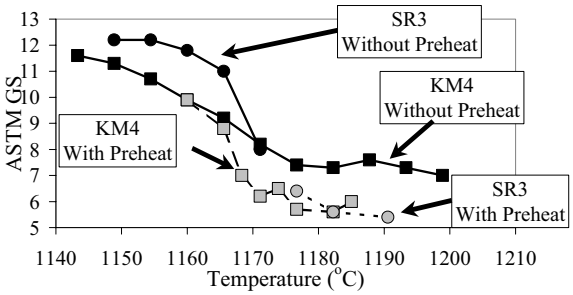

Figure 4
Grain Coarsening Response for SR3 and KM4

of a slightly coarser grain size (1 to 2 ASTM sizes) in the near and supersolvus regions.

To establish the effect of cooling rate on γ' size cubes approximately 2.5 cm on edge were sectioned and holes drilled to permit insertion of a thermocouple to measure cooling rates. Both sub-solvus and supersolvus heat treatments were conducted and temperatures recorded for KM4 and SR3 material. Cooling γ' size was measured using TEM replication techniques and results are summarized in Table VII and Figure 5.

Table VII. Effect of Temperature and Cooling Rate on the Distribution of Coarse and Fine Cooling γ'.

			Size (μm)		Area %		
	Temp[1]	Rate[2]	Crse[3]	Fine	Crse	Fine	Total
KM4	1191°C	17	.49	.04-.09	47.9	5.2	53.1
KM4	1191°C	46	.37	.03-.06	42.7	5.2	47.9
KM4	1188°C	88	.32	.06	44.8	2.1	46.9
SR3	1191°C	17	.41	.04-.07	40.6	6.3	46.9
SR3	1191°C	46	.28	.05	41.7	3.1	44.8
SR3	1185°C	87	.29	.06	35.4	4.2	39.6
KM4	1093°C	164	.71	.11	31.8	24	55.8
KM4	1093°C	43	.71	.04-.21	28.1	17.7	45.8
SR3	1096°C	157	.7	.09	21.4	21.9	43.2
SR3	1093°C	43	.68	.04-.18	37.5	15.6	53.1

1)Solution heat treatment temperature prior to cooling study.
2)Cooling rate from solution temperature to 871°C in °C/minute.
3)Coarse cooling γ'.

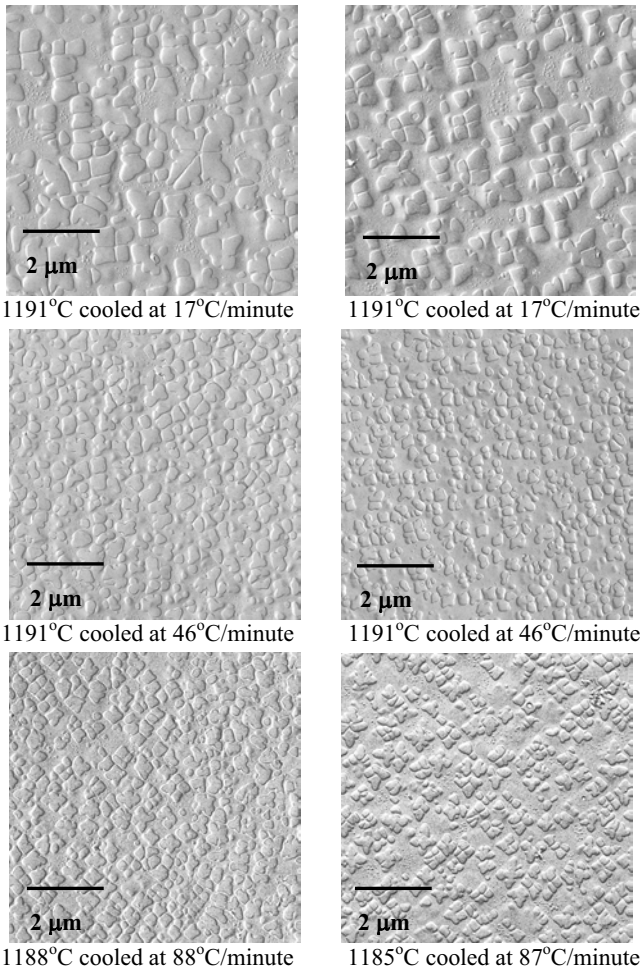

1191°C cooled at 17°C/minute 1191°C cooled at 17°C/minute
1191°C cooled at 46°C/minute 1191°C cooled at 46°C/minute
1188°C cooled at 88°C/minute 1185°C cooled at 87°C/minute

Figure 5
Observed cooling γ' distributions in KM4 (left) and SR3 (right).

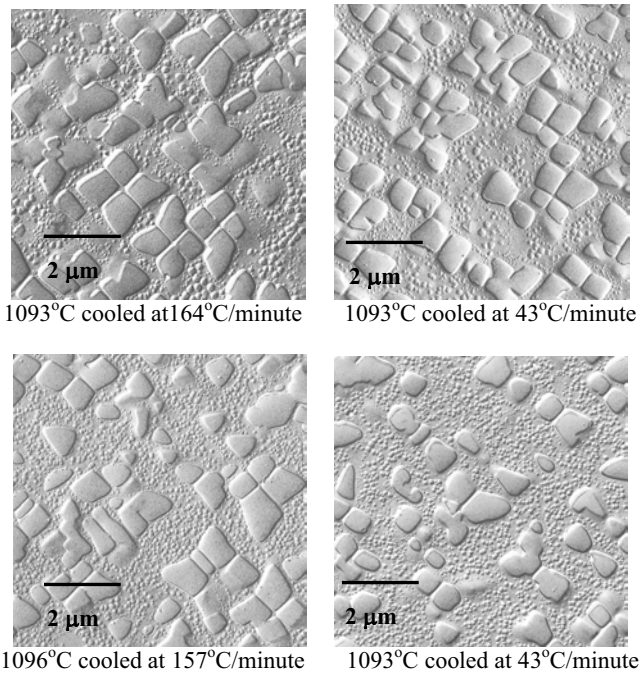

1093°C cooled at164°C/minute 1093°C cooled at 43°C/minute
1096°C cooled at 157°C/minute 1093°C cooled at 43°C/minute

Figure 5 (continued)
Observed cooling γ' distributions in KM4 (left) and SR3 (right).

Based on the work described above, the heat treatments listed in Table VIII (KM4) and IX (SR3) were defined to achieve the

Table VIII. KM4 Heat Treat Matrix Parameters. (footnotes in Table IX)

	Temp (°C)[1]		Cool Rate (°C/min)[2]		
Run	GC	Sltn	Aim	Meas	Stabil[3]
1	1193.3	1088	>111.1	194.4	871°C/2 hrs
2	1193.3	1177	<55.6	61.1	843 °C/4 hrs
3	1182.2	1088	<55.6	37.8	843 °C/4 hrs
4	1182.2	1177	>111.1	194.4	871 °C/2 hrs
5	1182.2	1177	>111.1	194.4	843 °C/4 hrs
6	1182.2	1127	<55.6	47.2	871 °C/2 hrs
7	1165.6	1166	<55.6	62.8	871 °C/2 hrs
8	1165.6	1127	>111.1	194.4	843 °C/4 hrs

Table IX. SR3 Heat Treat Matrix Parameters.

	Temp (°C)[1]		Cool Rate (°C/min)[2]		
Run	GC	Sltn	Aim	Meas	Stabil[3]
1	1193.3	1088	>111.1	138.3	none
2	1193.3	1177	<55.6	82.2	843 °C/4 hrs
3	1182.2	1088	<55.6	41.1	843 °C/4 hrs
4	1182.2	1177	>111.1	333.3+	none
4F	1182.2	1177	>111.1	178.9	none
5	1182.2	1177	>111.1	333.3+	843 °C/4 hrs
5F	1171.1	1171.1	>111.1	197.8	843 °C/4 hrs
6	1182.2	1118	<55.6	151.1	none
7	1171.1	1171	<55.6	87.8	none
8	1171.1	1118	>111.1	138.9+	843 °C/4 hrs

1) Grain Coarsening (GC) and Solution Heat treat Temperature.
2) Aim and measured cooling rate from solution heat treatment.
3) Stabilization heat treatment cycle.

desired microstructure. All heat treat runs were processed through a 760°C/8 hour age. Test blanks were heat treated and

thermocouples inserted into a heat treat block to record cooling rate of the test blanks. Examples of cooling rates measured for the

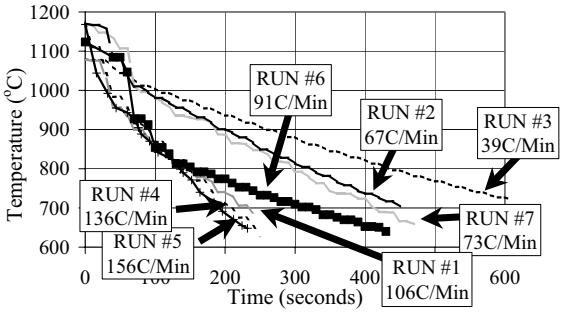

Figure 6
Measured Cooling Rates for SR3 Matrix Runs

SR3 heat treatments are presented in Figure 6. Measured cooling rates for each heat treatment run for the test matrix are also presented in Tables VIII (KM4) and IX (SR3). During processing two of the SR3 runs (run 4 and run 5) exhibited tendencies to notch sensitivity/cracking during processing (oil quenching of the blanks) and replacement material was heat treated with a slower cool to eliminate this behavior After heat treatment tensile, creep, and crack growth specimens were machined and testing conducted. All tests were conducted at 649°C with creep testing at 792.9 MPa and crack growth testing conducted using a 2 hour hold time at load under R = .1 conditions. All specimens were metallographically evaluated post test for grain size with one tensile specimen from each heat treat run submitted for TEM replication measurement of cooling γ' size and TEM thin foil measurement of aging γ' size by NASA.

Results

Test results are listed in Tables X (KM4) and XI (SR3) for the each of the microstructural variants. While crack growth rate curves were generated, data is reported as the measured da/dt at a maximum stress intensity of 33 MPa√meter. In addition, measured microstructures for each run are also listed. Typical microstructures for each of the experimental variations are presented in Figures 7 (KM4) and 8 (SR3). A quick review of the test results shows that microstructural variations can result in significant variations in material capability with yield and ultimate strengths varying by 117.2 and 144.8 MPa respectively for KM4. SR3 showed variations of 344.8 and 303.4 MPa. The larger variation for SR3 was due to the two runs that exhibited high strength and notch sensitivity. Excluding them from the assessment still showed SR3 to have greater sensitivity to microstructure with ranges of 193.1 and 200 MPa observed for yield and ultimate strengths. Ductility varied by a factor of 2 (14%) for KM4 and 2.5 (15%) for SR3. Creep life varied by 4X (120 to 840 hrs) for KM4 and three orders of magnitude (18 to 8039 hrs) for SR3. Crack growth rates varied by 3 orders of magnitude (1.52E-7 to 2.54E-4 m-sec^{-1}) for KM4 and four orders of magnituide {5.08E-7 to 2.54E-3) for SR3. On average the SR3 matrix exhibited better strength and creep capability and reduced crack growth resistance than the KM4 matrix. Excluding the two SR3 runs with exceptionally high strength, the SR3 matrix exhibited better ultimate and lower yield, significantly better creep and worse crack growth capability than the KM4 matrix. In all instances the SR3 variability was still greater. The major difference between the two matrices was the application of a stabilization heat treatment to each of the KM4 heat treatments and only half the SR3 heat treatment. In addition, the KM4 matrix generally showed lower variability than the SR3 matrix suggesting that the application of a stabilization cycle generally homogenizes the material properties.

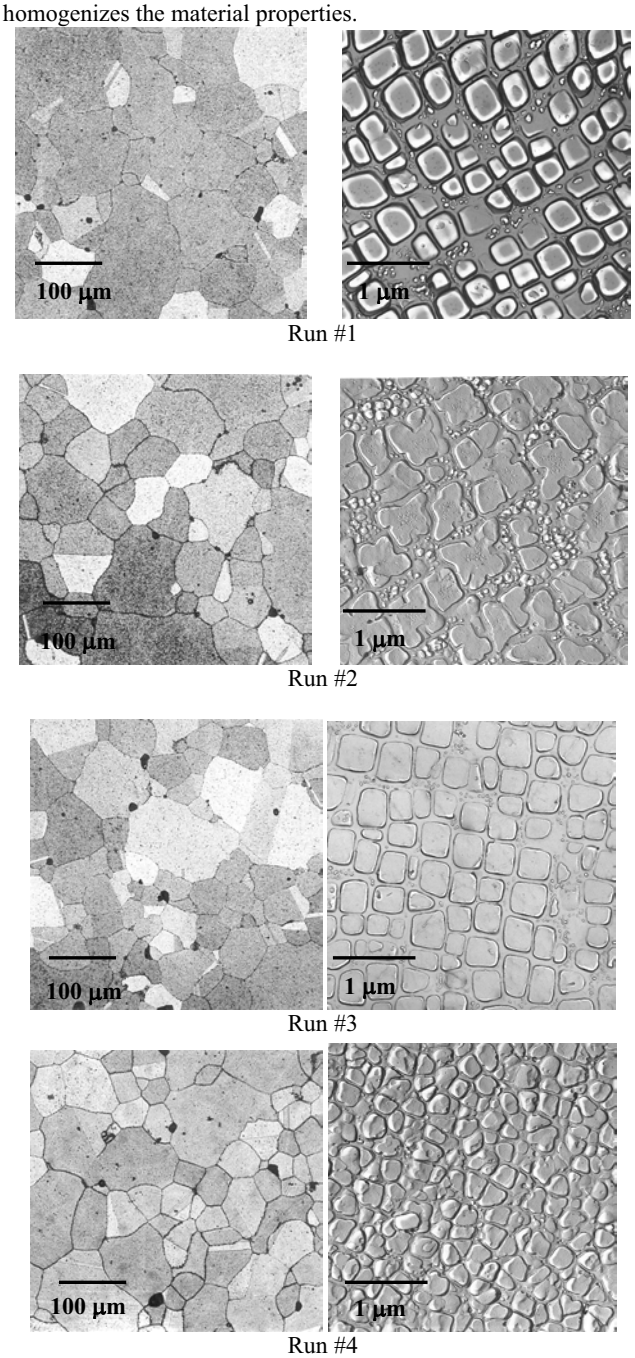

Figure 7
Typical Grain and γ' Structures Observed in KM4 Heat Treatment Study Runs 1 to 4.

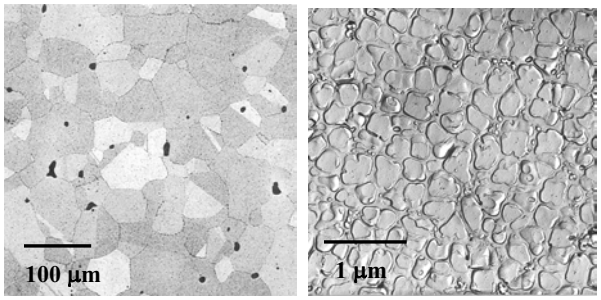

Run #5

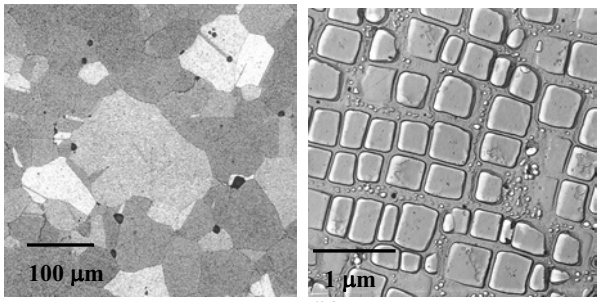

Run #6

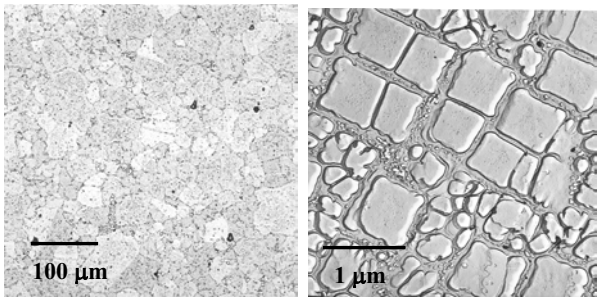

Run #7

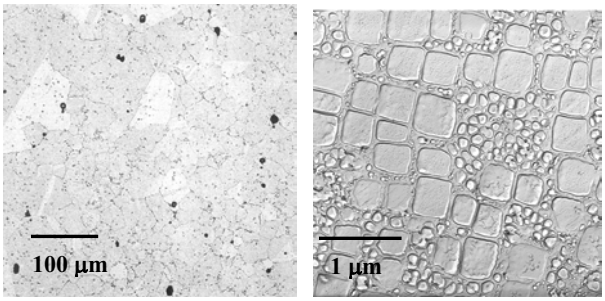

Run #8

Figure 7
Typical Grain and γ' Structures Observed in KM4 Heat Treatment Study Runs 5 to 8.

Review of the KM4 microstructures shows the presence of thermally induced porosity (TIP), multimodal γ' distributions and some evidence of incomplete solution (residual primary γ') for runs 7 and 8 which were heat treated very close to the γ' solvus.

Similar to the KM4 matrix, a wide variation in microstructure was also achieved for the SR3 heat treat studies. Compared to the KM4 materials a coarser grain size was achieved for runs one and two. In addition run #2 showed extensive TIP. Consistent with the KM4 materials multimodal and γ' distributions were observed. It should be noted that for both the KM4 and SR3 runs the desired distributions in cooling γ' size were not achieved. It appears that for the resolution heat treatments and subsequent cooling rates evaluated, coarsening of the stable γ' occurred rather than development of a higher volume fraction of finer cooling γ'.

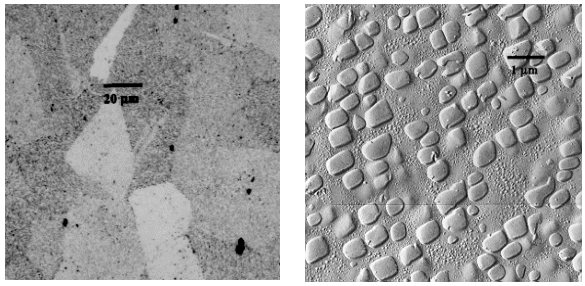

Run #1

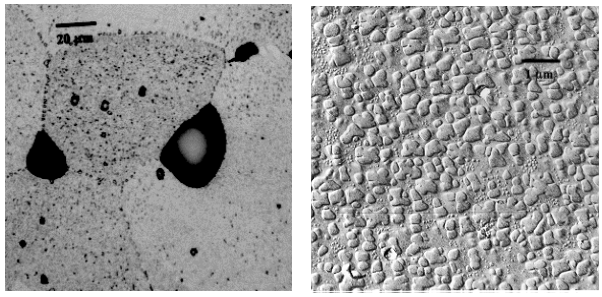

Run #2

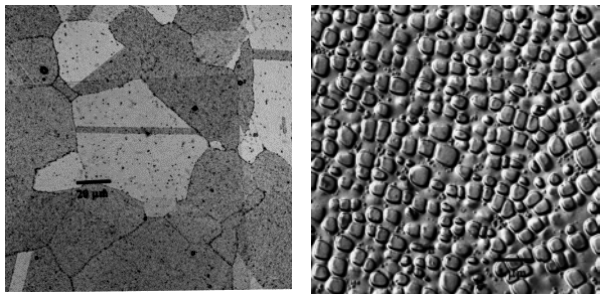

Run #3

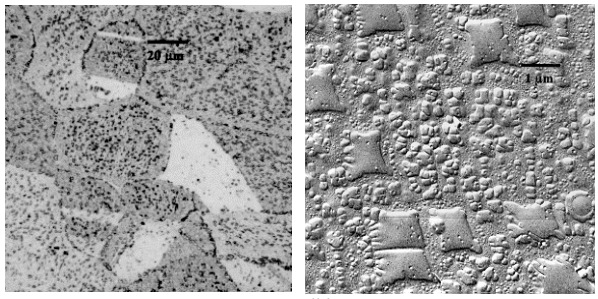

Run #4F

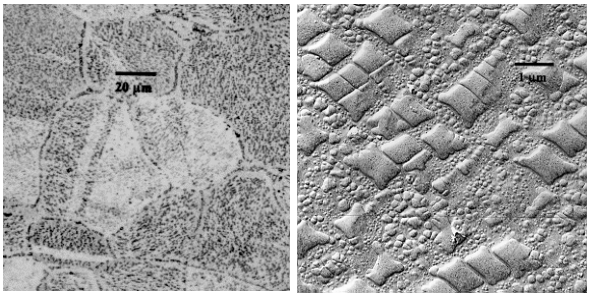

Run #5F

Figure 8
Typical Grain and γ' Structures Observed in SR3 Heat Treatment Study Runs 1 to 5F.

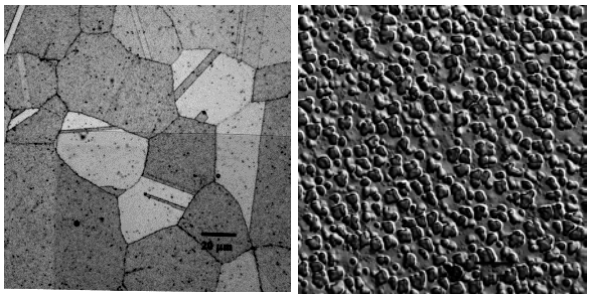

Run #6

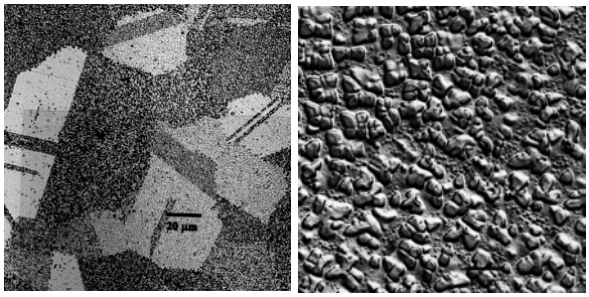

Run #7

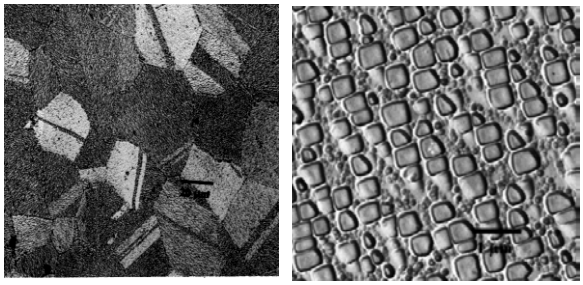

Run #8

Figure 8
Typical Grain and γ' Structures Observed in SR3 Heat Treatment Study Runs 6 to 8.

Table X. Test Results and Measured Grain Sizes for KM4 Matrix.

#[1]	GS[2]	YS[3]	UTS[4]	EL[5]	GS	Life[6]	GS	Da/dt[7]
1	4.4	956.3	1335.6	16.8	4.4	797	4.7	2.54E-7
1	4.4	972.2	1353.5	16.6	4.4	749	4.7	2.54E-7
2	4.6	960.5	1329.4	20.3	4.7	451	4.7	1.52E-10
2	4.6	931.5	1305.2	27.6	4.7	318	4.7	1.52E-10
3	5.3	930.1	1392.1	18	5.3	580	4.7	1.52E-7
3	5.3	932.2	1325.2	16.4	5.5	352	4.7	1.52E-7
4	5.4	1016.3	1459.7	16	5.3	726	5.4	1.78E-10
4	5.4	990.8	1413.5	17.5	5.8	582	5.4	1.27E-10
5	5.2	1025.3	1456.9	14.4	5.7	848	5	1.78E-10
5	5.2	997.7	1416.9	16.8	5.4	607	5	1.78E-10
6	5.1	909.5	1358.3	21.5	5.5	357	5	2.54E-7
6	5.1	969.4	1363.8	24.5	5.8	304	5	2.54E-7
7	5.9	1048	1416.2	28.2	6.2	122	7.4	3.81E-10
7	5.9	1043.2	1428.6	28.8	5.8	280	7.4	8.89E-10
8	7	1048	1416.2	25.7	7	707	6.2	3.81E-9
8	7	1043.2	1428.6	23.5	6.9	670		

1) Heat treatment run number (#)
2) Grain size measured in test specimen
3) .2 % Offset Yield strength (MPa)
4) Ultimate tensile strength (MPa)
5) Elongation (%)
6) Time to .2% creep at 649°C/793MPa
7) Crack growth rate in meters/second at a K_{max} of 33 MPa√m

Table XI. Test Results and Measured Grain Sizes for SR3 Matrix.

#[1]	GS[2]	YS[3]	UTS[4]	EL[5]	GS	Life[6]	GS	Da/dt[7]
1	3.2	953.6	1393.5	16.3	3.2	4288	3.4	2.54E-6
1	3.1	934.3	1383.1	15	3.7	5172	3.3	2.54E-6
2	2.1	839.8	1279	10.8	2.3	18	2.4	5.08E-10
2	2.5	860.5	1334.2	10	2.1	18.5	2.3	5.08E-10
3	6	879.8	1379	10.2	6.2	20	6	2.54E-6
3	6.2	896.4	1406.6	10.8	5.9	17.2	6	2.54E-6
4	5.9	1175.6	1523.1	12.1				
4F	5.7	994.3	1478.3	17.4	5.8	1446	6.1	2.54E-8
4F	6	998.4	1470	19	5.8	1350	6.5	2.54E-8
5	6.5	1148.7	1584.5	9.6				
5	6.8	1184.6	1567.2	7.3				
5F	5.6	933.6	1437.6	22.8	5.7	200	6.2	1.02E-9
5F	5.9	937.7	1421.7	24.9	5.8	401	6.4	5.08E-10
6	5.8	963.9	1480.4	17.1	5.7	8039	5.6	2.29E-9
6	5.7	992.9	1479	8.3	5.7	6550	5.6	2.29E-9
7	6.2	959.8	1446.6	17.2	5.6	753.3	6	5.08E-8
7	5.8	948.8	1437.6	22.2	6	854.3	5.8	5.08E-9
8	6.7	1026.7	1474.2	19.8	6.6	474	6.7	1.78E-9
8	6.5	1023.9	1470	19.5	6.6	549	6.4	6.35E-9

(see Table X for foot notes)

Cooling and aging γ' size was measured via TEM replication and TEM thin foil for one specimen from each of the heat treat runs and results are summarized in Table XII.

Table XII. Measured γ' Distributions for the SR3 (top) and KM4 (bottom) Matrix Runs.

	Cooling γ'		
HT #	Area %[1]	Size (μm) [1]	Age γ' (μm) [2]
1	34.9 & 14.6	.49 & .065	.027
2	43.8 & 4.7	.36 & .08	.044
3	42.3 & 6.6	.4 & .1	.041
4	42	.2	.017
4F	12.5, 28.1 & 8.9	1.1, .32 & .085	.045
5	43.5	.12	.037
5F	18.2, 17.7 & 8.9	1.7,.29 & .095	.057
6	40.5 & 7.1	.23 & .09	.015
7	36.1 & 13.9	.34 & .11	.051
8	33.3 & 21.1	.4 & .12	.057

(SR3)

	Cooling γ'		
HT #	Area %[1]	Size (μm) [1]	Age γ' (μm) [2]
1	48 & 6	.28 & .07	.046
2	57 & 9.4	.36 & .08	.03
3	54	.3	.025
4	67	.2	.038
5	63	.2	.035
6	59.6 & 5.1	.35 & .06	.064
7	33.3, 23.3 & 6.8	.33, .29 & .05	.04
8	40 & 31	.36 & .1	.063

1) Area % and size of γ' in order listed. For example SR3 run 1 has 34.9% at .29μm and 14.6% at .065 μm for a total area % of 49.5%.
2) Aging γ' size (area % not measured)

(KM4)

For analysis of the results of the test program, a weighted average cooling γ' was determined for each of the structures that developed a bimodal distribution. A summary of the weighted average cooling γ' sizes is presented table XIII.

Table XIII. Weighted Average Cooling γ' Sizes for KM4 and SR3 Runs.

	Weighted Average Cooling γ' Size (μm)	
Heat Treat Run	SR3	KM4
1	.365	.26
2	.333	.32
3	.36	.3
4	.1	.2
4F	.475	N/A
5	.12	.2
5F	.409	N/A
6	.21	.33
7	.28	.28
8	.29	.25

Analysis and Discussion

The original objective of the experimental matrices was to quantify the effect of microstructural variations on the 649°C capability of advanced, high strength P/M superalloys through the use of statistically based experimentation. However, this class of alloys represents a very complex material system resulting in significant material interactions. In the case of these studies one of the major interactions was associated with the effect of solution heat treat temperature and subsequent cooling rate on the cooling γ' distribution. Due to the slower cooling rates used in these experiments, the variation in relative volume fraction and size of cooling γ' was not controlled to the experimental levels desired. However, significant variation in microstructural features was achieved along with a corresponding range of mechanical properties. Because of the structure of the matrices it is possible to analyze the test results both with respect to microstructure as well as the heat treat steps through which the material was processed.

As a preliminary comparison, the average values for each of the microstructural features and tested mechanical properties were determined. The results are summarized below. For this exercise, two averages were calculated for the SR3 matrix; one with and one without the tensile data from the oil quench samples.

	GS	CGP	AGP	YS	UTS	EL	CRP	da/dt
KM4	5.4	.26	.045	973.4	1376	21	538	8.9E-8
SR3[1]	5.2	.34	.042	947	1423	16	1884	6.4E-7
SR3[2]	5.3	.33	.041	981.7	1444.5	15	1884	6.4E-7

1) Without run 4 and run 5 data
2) With run 4 and run 5 data
(see Tables X and XII for units)

In general the results show that on average the two alloys behave similarly with the greatest mechanical property variation between the two matrices being creep life and crack growth resistance with the SR3 matrix showing a faster growth rate and better creep capability than KM4. The primary difference between the two matrices beyond the compositional differences was that all heat treat runs of the KM4 matrix were processed through a stabilization heat treat cycle while only half the SR3 runs were processed with a stabilization heat treatment. This indicates that the use of a stabilization heat treatment reduces creep capability but improves the crack growth resistance of high volume fraction γ' P/M superalloys. More detailed analysis with respect to microstructural and processing effects are discussed in the following sections.

Effect of Microstructure The three microstructural features of interest for analysis of the test results are grain size and the size of both the cooling and aging γ'. Multi linear regression analysis of each of the test matrices individually and combined was conducted and statistically significant effects were identified. A summary of the effect of increasing each of these factors on the associated mechanical properties is presented below where "+" means the property is superior, "–" is inferior and "0" is no effect.

Feature	YS	UTS	Life	da/dt
Grain Size	-	-	0	0
Cooling γ' Size	-	-	-	0
Aging γ' Size	0	0	-	+

As expected the 649°C strength of both alloys increased with finer grain sizes and finer weighted average cooling γ' sizes. No effect of aging γ' size on strength was observed. Creep life did not appear to be strongly influenced by grain size and appeared to increase with refined cooling and aging γ' sizes. Crack growth rates did not appear to be affected by cooling γ' size but did appear to decrease with decreasing grain size and increasing aging γ' size. It should be noted that the grain size effect was not verified through regression analysis of the data. Of all the effects observed, the apparent effects on reducing dwell crack growth rate

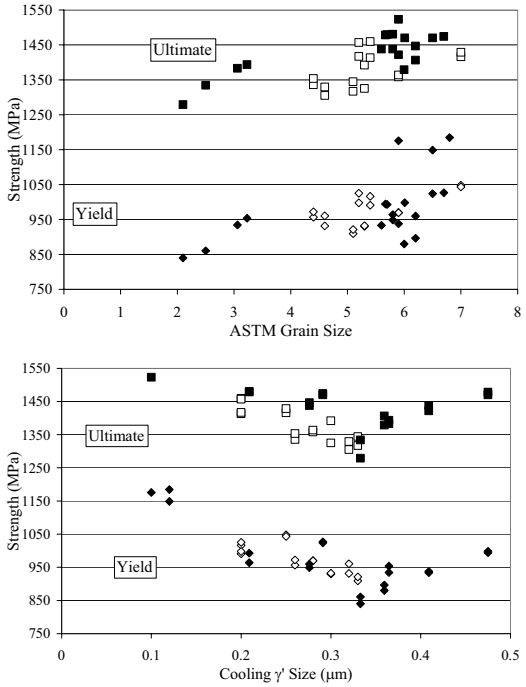

Figure 9
Effect of Grain Size & Cooling γ' Size on Strength (SR3-closed symbols and KM4-open symbols)

with increasing aging γ' size was the most unexpected. The tradeoff between creep and dwell crack growth capability suggests

that lower creep capability might result in some reduction in the driving force for growth at the crack tip during extended hold times. Additional work is required to more fully understand the mechanism associated with the observed behavior. Examples of each of the microstructural effects are presented in Figure 9.

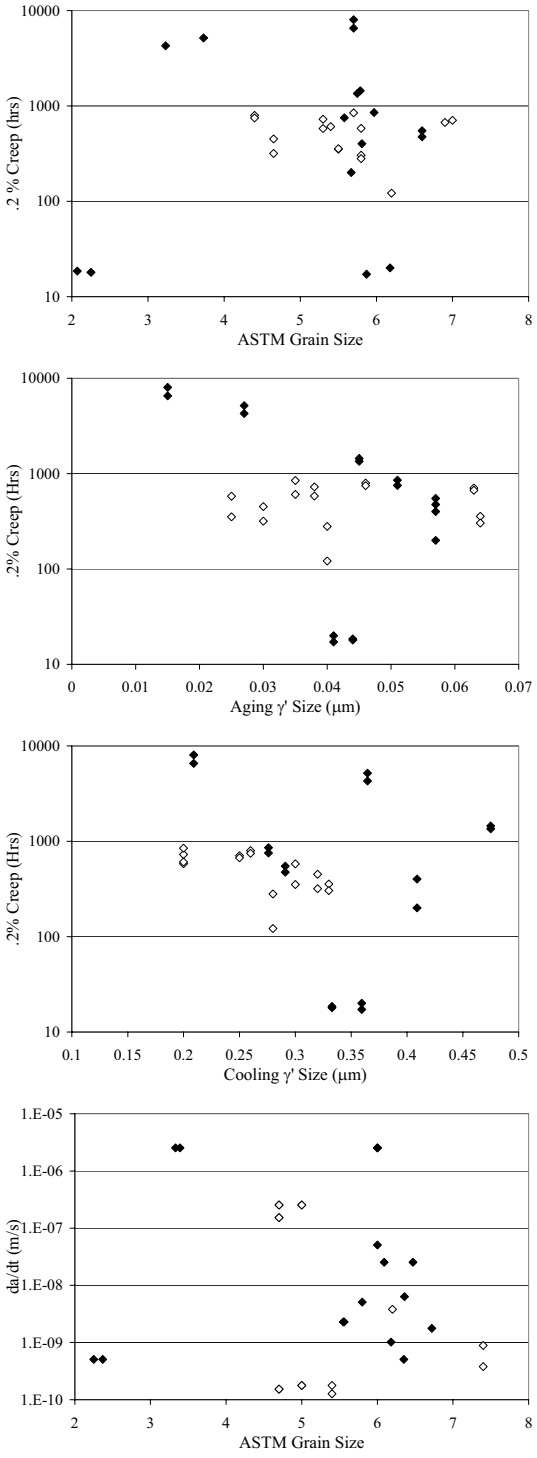

Figure 9 (continued)
Effect of Grain Size Aging γ' Size & Cooling γ' Size on Creep Life and Grain Size on Crack Growth Rate. (SR3-closed symbols and KM4-open symbols)

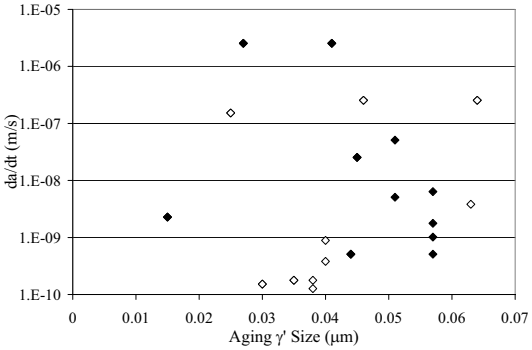

Figure 9 (continued)
Effect of Aging γ' Size on Crack Growth Rate (SR3-closed symbols and KM4-open symbols).

Effect of Heat Treatment. For the purposes of analyzing the processing parameters it was assumed that the effect of the grain coarsening heat treat temperature was significantly reduced by the subsequent processing so the three parameters selected for analysis were solution heat treat temperature, cooling rate from solution and stabilization cycle. For the SR3 runs not processed with a stabilization cycle, the age temperature was used for the analysis. The summary of the regression analysis is presented below where the effect of increasing the variable listed on the property of interest is reported as inferior (-), superior (+) or no effect (0).

Parameter	YS	UTS	Creep	da/dt
Solution Temperature	0	0	-	+
Cooling Rate	+	+	0	0
Stabilization Temperature	0	-	-	0

The results clearly show that there is a need to select the heat treatment to achieve the optimum property balance. Plots of the various effects are presented in Figure 10. As expected, cooling rate strongly influenced the strength of the material. Surprisingly solution temperature strongly influenced crack growth resistance. While not statistically significant, it appears as if stabilization temperature influences both the crack growth and creep capability of the material.

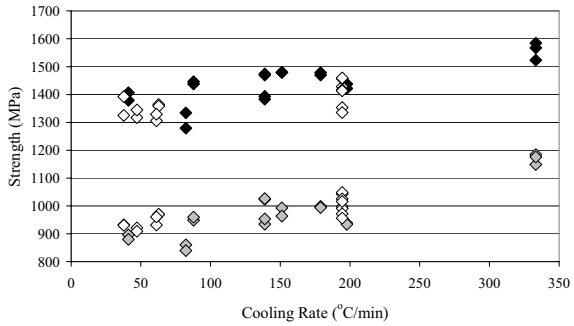

Figure 10
Effect of Cooling Rate from Solution Heat Treatment on Strength (SR3-closed symbols and KM4-open symbols). Light gray symbols are YS, black symbols are UTS.

It is readily apparent that heat treat processing can be tailored to achieve the optimum balance of high temperature properties. For an application requiring a balance of good high temperature strength, creep and crack growth resistance the results suggest that solution heat treating supersolvus, followed by an aggressive cooling rate is desirable. Selection of the stabilization temperature is strongly dependent upon the balance of creep and crack growth capability desired as well as other producibility considerations.

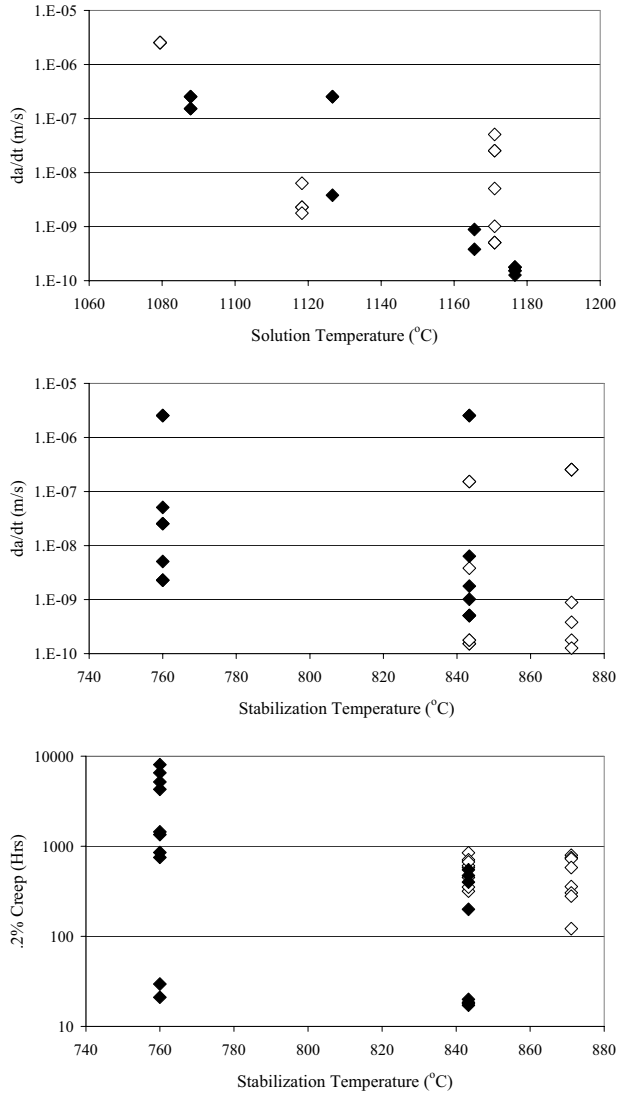

Figure 10 (continued)
Effect of Solution and Stabilization Heat Treat Temperatures on Creep Life and Stabilization Temperature on Crack Growth Rate. (SR3-closed symbols and KM4-open symbols)

Summary

A systematic evaluation of the effect of microstructure on the elevated temperature property balance was conducted demonstrating that the property balance of high strength PM disk superalloy materials can be significantly affected by the heat treatment applied and microstructures developed. For a desired combination of good high temperature capability the results indicate that a supersolvus heat treatment followed by a fast cooling rate is desired. In addition, selection of a stabilization heat treat cycle would depend upon the balance of creep and crack growth capability desired.

Acknowledgements

The authors gratefully acknowledge the financial support of NASA Glenn Research Center, under Government contract NAS3-26385. The sustained effort and effective team approach between NASA and both contractors for the High Speed Civil Transport – EPM program led to significant advances in understanding relationships between P/M superalloy composition and processing and high temperature, long dwell properties. For NASA, Robert Draper was the focal point for the majority of the program; Draper was assisted by many colleagues, in particular Tim Gabb and Jack Telesman. The authors also acknowledge support of many colleagues including Bob Van Stone, Joseph Heaney, Ron Tolbert and David Miller of GE; Herb Chin and Jerry Capo of P&W; Jennifer Heine, formerly of P&W and now at GE; and Mei Ling Henne, formerly of P&W and now at PCC.

References

1) A. Manonukul, F. P. E. Dunne, D. Knowles; "Physically-based model for creep in nickel-base superalloy C263 both above and below the gamma solvus"; Acta Materialia 50 (2002) 2917-2931
2) K. R. Bain, M. L. Gambone, J. M. Hyzak, M. C. Thomas; "Development of Damage Tolerant Microstructures in Udimet 720"; Superalloys 1988; The Minerals, Metals & Materials Society; 1988; edited by Reichman et al
3) P. R. Bhowal, E. F. Wright, and E. L. Raymond, "Effects of Cooling Rate and γ' Morphology on Creep and Stress Rupture Properties of a Powder Metallurgy Superalloy", Met. Trans., 21A, 1990, pp. 1709-1717.
4) D. D. Krueger, J. F. Wessels, K. M. Chang; US Patent 5,143,563; "Creep, Stress Rupture and Hold Time Fatigue Resistant Alloys"; September 1, 1992
5) E. S. Huron, K. R. Bain, D. P. Mourer, J. J. Schirra, P. L. Reynolds, E. E. Montero; "The Influence of Grain Boundary Elements on Properties and Microstructures of P/M Nickel Base Superalloys"; elsewhere in these proceedings
6) D. P. Mourer, E. Raymond, S. Ganesh, J. Hyzak; "Dual Alloy Disk Development"; Superalloys 1996; The Minerals, Metals & Materials Society; 1996; edited by Kissinger, et al; pgs 637-643